Carbohydrate Polymers 291 (2022) 119611

Contents lists available at ScienceDirect

Carbohydrate Polymers

journal homepage: www.elsevier.com/locate/carbpol

Chitosan sulfate-lysozyme hybrid hydrogels as platforms with fine-tuned degradability and sustained inherent antibiotic and antioxidant activities

Antonio Aguanell, María Luisa del Pozo, Carlos Pérez-Martín [1], Gabriela Pontes, Agatha Bastida, Alfonso Fernández-Mayoralas, Eduardo García-Junceda *, Julia Revuelta *

BioGlycoChem Group, Departamento de Química Bio-Orgánica, Instituto de Química Orgánica General, CSIC (IQOG-CSIC), Juan de la Cierva 3, 28006 Madrid, Spain

ARTICLE INFO

Keywords:
Chitosan sulfate
Lysozyme
Polymers
Physicochemical parameters
Antibiotic activity
Antioxidant activity

ABSTRACT

The control of the properties and biological activities of chitosan-lysozyme hybrid hydrogels to exploit their interesting biomedical applications depends largely on the chitosan acetylation pattern, a difficult parameter to control. Herein, we have prepared sulfated chitosan-lysozyme hydrogels as versatile platforms with fine-tuned degradability and persistent bactericidal and antioxidant properties. The use of chitosan sulfates instead of chitosan has the advantage that the rate and mechanisms of lysozyme release, as well as antibacterial and antioxidant activities, depend on the sulfation profile, a structural parameter that is easily controlled by simple chemical modifications. Thus, while 6-*O*-sulfated chitosan hydrogels allow the release of loaded lysozyme in a short time (60% in 24 h), due to a high rate of degradation that allows rapid antibiotic and antioxidant activities, in 3-*O*-sulfated systems there is a slow release of lysozyme (80% in 21 days), resulting in long-lasting antibiotic and antioxidant activities.

1. Introduction

Chitosan hydrogels are three-dimensional (3D) networks formed by physical or chemical cross-linking of this sustainable polymer derived from abundant renewable resources (Domalik-Pyzik et al., 2019). The diverse biological activities of chitosan (analgesic, antitumor, anti-inflammatory, antimicrobial, etc.) combined with various bioactive properties such as non-toxicity, biodegradability, absorbability and others, as well as its excellent ability to form hydrogels, have led to the use of this polymer for the preparation of hydrogels for biomedical applications (Eivazzadeh-Keihan et al., 2022), including drug delivery (Peers et al., 2020), tissue engineering (Pita-López et al., 2021), wound dressing (Liu et al., 2018a), and so on. Several studies have shown that chitosan-based hydrogels further improve their properties when chemically modified by covalent conjugation and/or combined with small molecules, other polymers, proteins, nanocomposites, or cells (Nicolle et al., 2021; Sanchez-Salvadoret al., 2021; Torkaman et al., 2021).

Lysozyme, a glycoside hydrolase with high enzymatic specificity for the hydrolysis of the glycosidic bonds of chitosan (Tomihata & Ikada, 1997), is widely used to modulate the properties of chitosan-based biomaterials, such as degradation (Lončarević et al., 2017) and to improve the profiles of controlled-release drugs (Herdiana et al., 2022). In addition, antibacterial films prepared by incorporating lysozyme into chitosan were reported not only to retain lysozyme activity but also to enhance the antimicrobial ability of lysozyme (Li et al., 2017). This enhancement of antibacterial activity was attributed not only to the release of lysozyme, but also to a possible synergistic effect between chitooligomers and lysozyme obtained after chitosan hydrolysis (Kim et al., 2020; Saito et al., 2019). Finally, chitosan and lysozyme represent a versatile combination to create porous structures by degrading hydrogels. These spaces promote cell proliferation and migration and contribute to osteogenic differentiation when mesenchymal stem cells are encapsulated in chitosan-lysozyme hydrogels (Kim et al., 2018).

These results suggest that the strategy of combining lysozyme with chitosan may be a promising approach to improve not only the functionalities of chitosan-based hydrogels but also their biomedical applications. However, despite the above advantages, the combination of chitosan and lysozyme in these systems also has important drawbacks.

On the one hand, the interaction between chitosan and lysozyme strongly depends on the degree of acetylation of the chitosan (DA), and

* Corresponding authors.
E-mail addresses: aaguanel@ucm.es (A. Aguanell), mluisa.delpozo@csic.es (M.L. del Pozo), UO279482@uniovi.es (C. Pérez-Martín), agatha.bastida@csic.es (A. Bastida), mayoralas@iqog.csic.es (A. Fernández-Mayoralas), eduardo.junceda@csic.es (E. García-Junceda), julia.revuelta@iqog.csic.es (J. Revuelta).
[1] Present address: Departamento de Química Orgánica e Inorgánica, Universidad de Oviedo, Julián Clavería 8, 33006 Oviedo, Spain.

https://doi.org/10.1016/j.carbpol.2022.119611
Received 23 February 2022; Received in revised form 6 May 2022; Accepted 9 May 2022
Available online 12 May 2022

low degrees of acetylation have been associated with low affinities between lysozyme and the polysaccharide (Nordtveit et al., 1996). However, a high degree of acetylation negatively affects the solubility of chitosan, a crucial property not only for handling in the manufacture of materials but also for use in biomedical applications (Pillai et al., 2009). Moreover, the solubility properties of chitosan depend not only on its average degree of acetylation but also on the distribution of acetyl groups along the chain, and a block distribution of acetylation residues significantly reduces the solubility of the polymer (Kurita et al., 1991). Nevertheless, commercial chitosan is mainly prepared by chemical deacetylation of chitin under heterogeneous conditions, resulting in polymers in which the acetyl groups are distributed in blocks with a random acetylation pattern (Weinhold et al., 2009).

On the other hand, it has been described that the substrate specificity of lysozyme with respect to chitosan is related to specific acetylation sequences. Lysozyme has a binding site that can accommodate a hexasaccharide sequence with three or more acetylated units, whereas it does not act on sequences characterized by a lower proportion of acetylated residues (Song et al., 1994). In addition, it is known that chitosan with a low degree of deacetylation can act as an inhibitor of lysozyme (Vårum et al., 1996). Although better defined, less dispersed chitosan with non-random acetylation patterns is already obtained at laboratory scale (Cord-Landwehr et al., 2020; Wattjes et al., 2019, 2020), further research is needed to develop high-yield- and cost-effective protocols for tailoring polymers with specific acetylation sequences.

Chemical modification of chitosan offers a great opportunity to develop solutions for a wide range of biomedical and technological applications (Nicolle et al., 2021). In this sense, the modification of chitosan with sulfate groups has attracted increasing attention in recent decades, as it confers new and attractive physicochemical properties to polymers compared to the starting chitosan, as well as interesting pharmacological properties and biological activities (Revuelta et al., 2021). Advances in chemo- and/or regioselective chitosan sulfonation and physicochemical characterization (Bedini et al., 2017) have paved the way for the development of sulfated chitosan-based entities with a wide range of possibilities. Nevertheless, successful process optimization and development of these entities is currently only possible by understanding how the specific structural properties of chitosan sulfates, especially the sulfation profile, determine their functionalities and biological activities. In this context, one of the most important challenges is to identify the role of chemistry, structure, and the understanding and use of these roles in biomedical applications. Recent advances in this field have focused mainly on deciphering the structural determinants of the so-called heparanized chitosans, a very interesting family of polysaccharides that have shown the ability to mimic heparan sulfates and heparin as ligands of various proteins, thereby exerting their biological activity by mimicking the function of these glycosaminoglycans (Doncel-Pérez et al., 2018; Revuelta et al., 2020). Morever, some progress has been made in the last decade in the binding of lysozyme to chitosan sulfates. In particular, regioselectively sulfated chitosans have been described to have differential effects not only on their protein binding affinity and specificity, but also on lysozyme activity (Wang et al., 2012; Yuan et al., 2009).

Based on the above, we hypothesize that the preparation of hydrogels based on chitosan sulfates and lysozyme can be a versatile alternative to chitosan-lysozyme backbones. Our hydrogels offer versatile platforms with fine-tuned degradability and persistent bactericidal and antioxidant properties. The use of chitosan sulfates instead of chitosan has the advantage that the rate and mechanisms of lysozyme release, as well as antibacterial and antioxidant activities, depend on the profile of sulfation along the chains, a structural parameter that, unlike the degree of acetylation and the presence of specific acetylation sequences, can be easily controlled by simple chemical modifications (Bedini et al., 2017). Finally, our study also addresses the question of how the chitosan sulfate structures control the behaviour of the hydrogels upon addition of lysozyme.

2. Materials and methods

2.1. Materials

Chitosan (CS) (degree of deacetylation 85%; molecular weight 50–150 kDa) was purchased from IDEBIO, S.L. (Spain) and purified before use (Nakal-Chidiac et al., 2020). Briefly, **CS** (5.0 g) was dissolved in a 0.5 M solution of acetic acid in water (1 L), and the solution was stirred for 24 h, keeping the pH between 4.0 and 4.5 by adding acetic acid as needed. The solution was then filtered to remove undissolved particles, and CS was precipitated again with an aqueous NaOH solution (10% w/v) until the pH = 8. The resulting suspension was centrifuged (15 min, 3900 rpm) and the supernatant was removed, with the remaining solid washed with an EtOH/H_2O mixture (70:30 v/v → 50:50 v/v → 30:70 v/v → 0:100) (400 mL). The resulting solid was finally resuspended in H_2O and lyophilized. All reagents were commercially available and were used without further purification. For statistical analysis, an unpaired *t*-test was performed.

2.2. Synthesis of chitosan sulfates

We synthesized 2-*N*-sulfated (**2S-CS**), 3-*O*-sulfated (**3S-CS**), 6-*O*-sulfated (**6S-CS**), and 3,6-*O*-disulfated (**3,6S-CS**) chitosan according to previously described procedures (Han et al., 2016; Holme & Perlin, 1997; Kariya et al., 2000; Zhang et al., 2010). Detailed procedures are described in the Supplementary Information.

2.3. Characterization of chitosan sulfate samples

^{1}H NMR, ^{13}C NMR and 2D (^{1}H—^{13}C HSQC) spectra were registered on a Varian Unity Inova 500 MHz spectrometer.

The degree of acetylation (DA) was calculated from ^{1}H NMR according to the method described by Jiang et al. (2017), using Eq. 1:

$$\mathrm{DA}\ (\%) = \frac{3 \times A_2}{6 \times A_1} \times 100 \tag{1}$$

where A_1 are the protons integral values of positions C_2–C_6 on the sugar ring and A_2 are the protons integral values of the three *N*-acetyl protons of the *N*-acetyl-D-glucosamine units.

The total degree of sulfation (DS) was determined from the sulfur (% S) and nitrogen (%N) content determined by elemental analysis using a Heraus CHN-O analyzer (Doncel-Pérez et al., 2018), and the calculation was performed according to Eq. 2:

$$\mathrm{DS} = \frac{\mathrm{S\%}/32.06}{\mathrm{N\%}/14.01} \tag{2}$$

ζ-Potentials determinations were performed using a Malvern Zetasizer Nanoseries Nano ZS instrument. Chitosan sulfate samples were dissolved at 1 mg/mL in 1 mM NaCl. Three replicates of each sample were performed.

2.4. Preparation of hydrogels

Hydrogels were prepared according to Akakuru and Isiuku (2017) procedure with modifications. Briefly, chitosan sulfate samples (≈1.2 mmol of repeating unit) were dissolved in 10 mL of 0.5% (v/v) aqueous acetic acid at room temperature with constant stirring for 24 h to obtain pale yellow viscous solutions. The solutions were then filtered using a sintered glass crucible and a 4% (v/v) aqueous glutaraldehyde solution was added (1 mL for 6S-CS, 3S-CS and 2S-CS or 2.5 mL for 3,6S-CS). The obtained solutions were then poured into Petri dishes and dried overnight at room temperature to form the crosslinked hydrogels. When the hydrogels were semi-dried, they were first washed with an aqueous 1.0 M NaOH solution and then with H_2O until the supernatant had a neutral pH. The hydrogels were then cut into small disks with a diameter of 20

mm and a height of 2 mm and dried in an oven at 35 °C for 48 h to completely remove the remaining solvent and obtain xerogel films (Alemán et al., 2007) with a thickness between 30 and 45 μm, depending on the polysaccharide used (see Fig. S1).

2.5. Swelling behaviour

The swelling ratio of the hydrogel was determined by a gravimetric method (Kim et al., 2020). The stored hydrogel disks were weighed (*Wd*) and then immersed in 10 mL solutions with different pH values (3.5, 7.2 and 9.0) for 48 h at 25 °C, and then weighed again (*Ws*). Finally, the swelling ratio was quantified using Eq. 3:

$$\text{Swelling ratio } (S)\ (\%) = \left(\frac{Ws - Wd}{Wd}\right) \times 100 \quad (3)$$

2.6. Lysozyme absorption into hydrogels

Xerogel disks (ø = 2 cm) were transferred to a vial containing 2.5 mL of lysozyme solution (10 mg/mL) in Tris-HCl 200 mM buffer (pH = 3.5) and allowed to adsorb protein for 72 h in a shaker (37 °C, 50 rpm). The protein solution was removed from the vial and analysed using a NanoDrop™ One C microvolume UV-VIS spectrophotometer equipped with a Protein A_{280} application for lysozyme determination which assumes that the molar extinction coefficient of the protein at 280 nm is 36,000 M^{-1} cm^{-1}. Finally charged-disks were vacuum-dried for 4 h.

2.7. Lysozyme binding activity of polysaccharides

The lysozyme binding activity of **CS** and chitosan sulfates (**3,6S-CS**, **2S-CS** and **6S-CS**) was measured based on the lysozyme–polysaccharides flocculation formation activity according to a previously described procedure (Yuan et al., 2009). A detailed description of the procedure can be found in the Supporting Information.

2.8. Hydrogels degradation

The degradation of the hydrogels was analysed using a gravimetric method, in which the change in dry weight was measured 7 and 14 days after incubation in distilled water. The change in dry weight was quantified using Eq. 4:

$$\text{Hydrogel degradation } (\%) = \frac{(W_i - W_t)}{W_t} \times 100 \quad (4)$$

where W_i and W_t indicate the dry weight at the beginning and at the respective time points.

2.9. Morphological observation of hydrogels

The morphological changes of hydrogels after contact with lysozyme were observed by scanning electron microscopy using a Hitachi S-8000 (Tokyo, Japan) operating in transmission mode at 100 kV on dry samples.

2.10. Releasing of lysozyme from chitosan sulfate hydrogels

Loaded xerogels were washed with Tris-HCl 200 mM buffer (pH = 7.0) for 5 min and then transferred to a vial containing 2.5 mL of this same buffer. The vial was kept in a shaker (37 °C, 50 rpm) throughout the experiment. The experiments were also performed in water with different pH values (3.5 and 9.0). To measure the lysozyme concentration, 5 μL of the supernatant were taken at different times. The amount of lysozyme was determined using the Protein A280 application of the NanoDrop™ One C microvolume UV-VIS spectrophotometer.

The values were fitted to the Korsmeyer-Peppas model according to Eq. 5:

$$F = Kt^n \quad (5)$$

where F is the drug release fraction at time t (F = Mt / M∞) in which Mt is the drug-released percentage at time t and M∞ is the total drug-release percentage. Time has been normalized as t/t∞ where t∞ is the total experiment time. The exponent "n" is known as "diffusional exponent" and is related to the release mechanism, being obtained from the plot of ln (F) versus ln (t).

2.11. Lysozyme binding to sulfated chitosans by surface plasmon resonance (SPR)

The surface of a CM5 sensor chip (Biacore Inc., GEHealthcare, Boston, MA, USA) was activated with a freshly mixture of *N*-hydroxysuccimide (NHS; 100 mM) and 1-(3-(dimethylamino) propyl)-ethylcarbodiimide (EDC; 400 mM) (1/1, v/v) in water. Lysozyme (50 μg/mL) in aqueous NaOAc (10 mM, pH 5.0) was then passed over the surface until a ligand density of 7000 RUs was reached. Quenching of the remaining active esters was achieved by passing aqueous ethanolamine (1.0 M, pH 8.5) over the surface of the chip. The control flow cell was activated with NHS and EDC and then treated with ethanolamine. HBS-EP buffer (0.01 M HEPES, 150 mM NaCl, 3 mM EDTA, 0.05% polysorbate 20; pH 7.4) was used as the running buffer for immobilization, binding, and affinity analysis. A concentration of 1 mg/mL of each compound in HBS-EP buffer at a flow rate of 30 μL/min and a temperature of 25 °C was used for the experiments. A 30 s injection of aqueous NaCl (2.0 M) at a flow rate of 30 μL/min was used for regeneration to reach the initial condition. Analysis was performed using BIAcore X100 analysis software (Biacore Inc., GE Healthcare, Boston, MA, USA).

2.12. Measurement of lysozyme activity by determination of reducing sugars using the 3,5-dinitrosalicylic acid (DNS) method

Solutions of chitosan sulfates (4% *w/v*) in H_2O (0.5 mL) were mixed with 0.5 mL of a lysozyme solution (2% w/v) (both solutions were preheated at 50 °C for 5 min before mixing). After 2, 4, 6, or 24 h of incubation at 50 °C, an aliquot of the mixtures (10 μL) was taken and heated at 100 °C for 8 min to stop the reaction. The mixture was then centrifuged and the supernatant was analysed by DNS-assay (Fig. S2) (Gusakov et al., 2011). Briefly, 30 μL of DNS reagent (1 g of 3,5-dinitrosalicylic acid, 3 g of sodium/potassium tartrate in 80 mL of 0.5 M NaOH by heating and stirring at 70 °C) was added to the test aliquot and the mixture was incubated in a boiling water bath for 5 min. After cooling to room temperature, the absorbance of the supernatant was measured at 540 nm. The A_{540} values for the substrate and enzyme blank values were subtracted from the A_{540} value for the analysed sample. The substrate and enzyme blanks were prepared in the same manner as the analysed sample except that 0.5 mL of the acetate buffer was added to the substrate (enzyme) solution instead of the enzyme (substrate) solution.

2.13. Antimicrobial activity

Fresh cultures of *E. coli* were grown by suspending one colony from the LB -agar culture in 5 mL of sterile LB medium and incubating for 24 h at 37 °C with constant shaking (136 rpm). Four falcons (50 mL) were then inoculated with 5 mL of sterile LB medium with the amount of bacterial culture required for an initial OD_{600} of 0.05. One falcon served as a control and was used to determine the total number of colonies in the culture. To each of the other three falcons, a lysozyme solution (33 μL, 0.3 μg/mL) and disks (ø = 2 cm) of xerogel without or with lysozyme were added. After incubation at 37 °C with constant shaking (90 rpm), the growth of the cultures was monitored until the exponential growth phase (OD_{600} of 0.3–0.4) was reached. The obtained bacterial suspensions were serially diluted and different dilutions (10^{-4}, 10^{-5} and 10^{-6} cfu mL^{-1}) were seeded on nutrient agar to determine the number of

viable bacteria and quantify the number of colony forming units (cfu mL^{-1}). Inhibition of colony formation (%) was determined using Eq. 6:

$$\text{Inhibition of colony formation } (\%) = \frac{\text{cfu}_{exp}}{\text{cfu}_{cont}} \times 100 \quad (6)$$

where cfu_{exp} and cfu_{cont} indicate cfu mL^{-1} of the experimental and control groups, respectively.

The hydrogels were then removed from the falcon tubes and the cultures centrifuged at 4000 rpm for 10 min, discarding the pellet. The hydrogels and a new lysozyme solution (33 μL, 0.3 μg/mL) were returned to the falcons, and the amount of bacterial cultures required for an initial OD_{600} of 0.05 was added, and the procedure described above was repeated to determine the number of colony-forming units (cfu mL^{-1}). The same protocol was repeated for 3 consecutive days.

2.14. Antioxidant activity: DPPH-radical scavenging ability assay

Disks (ø = 2 cm) of each xerogel without lysozyme were immersed in 4 mL of 0.1 mM DPPH (2,2-diphenyl-1-picryl-1-hydrazyl-hydrate) methanol solution. A 0.1 mM DPPH methanol solution (4 mL) without xerogel was used as control. The solutions were kept in the dark and the absorbance of the solution at 517 nm was determined at intervals of 1 h to 24 h.

In addition, disks (ø = 2 cm) of each lysozyme-incorporated xerogel were immersed in 5 mL Tris-HCl buffer (200 mM; pH = 7.0) and kept in a shaker (37 °C, 50 rpm) for 72 h. Aliquots of the supernatant solution (0.5 mL) were taken at 24 to 72 h intervals and incubated with water (0.5 mL) and DPPH (2 mL) at 25 °C for 30 min. The concentration of DPPH was 120 μM in the test solution. Then, the absorbance of the remaining DPPH radical was measured at 517 nm against a blank.

The scavenging effect was calculated according to Eq. 7:

$$\text{Scavenging effect } (\%) = \left[1 - \frac{A_{sample\ 517\ nm} - A_{control\ 517\ nm}}{A_{blanck\ 517\ nm}}\right] \times 100 \quad (7)$$

where $A_{sample\ 517nm}$ represents the absorbance of the sample at 517 nm, $A_{blank\ 517nm}$ represents the absorbance of the blank at 517 nm and $A_{control\ 517nm}$ represents the absorbance of the control (distilled water instead of DPPH) at 517 nm.

3. Results and discussion

3.1. Synthesis and characterization of chitosan sulfates

We prepared 2-*N*-sulfated (**2S-CS**) (Holme and Perlin, 1997), 3-*O*-sulfated (**3S-CS**) (Kariya et al., 2000), 6-*O*-sulfated (**6S-CS**) (Han et al., 2016) and 3,6-*O*-di-sulfated (**3,6S-CS**) (Zhang et al., 2010) chitosan according to previously published procedures. Elemental analysis showed that the degree of sulfation (DS) ranged from 0.7 to 1.7 (Table 1).

The regioselectivity of the sulfations was analysed by ^{13}C NMR experiments (Fig. 1a and Table 2). After 6-sulfation, the 59.3 ppm signal of C_6(OH) in chitosan was shifted down to 66.5 ppm in sulfated chitosan, representing the ^{13}C signal of $C_6(SO_3^-)$ in **6S-CS**. On the other hand, the appearance of the 73.9 ppm signal $C_3(SO_3^-)$ and the partial disappearance of the 69.9 ppm signal C_3(OH) indicate that the hydroxyl group at C_3 in the **3,6S-CS** was sulfated. In addition, the complete disappearance of the 67.7 ppm signal and the appearance of the 61.4 ppm signal C_6(OH) indicated that position 6 of **3,6S-CS** in the **3S-CS** was completely 6-*O*-desulfated. Finally, the data shown in Fig. 1a indicated that position 2 of chitosan in **2S-CS** was regioselectively sulfated.

The ratio of sulfated to non-sulfated residues was determined by integrating each array/body of signals with respect to the CH-2 density of DEPT-HSQC spectra to estimate the degree of sulfation.

In doing so, we assumed that the compared signals had similar values of the $^1J_{CH}$ coupling constant and that differences of about 5–8 Hz from the experimental value did not cause a significant deviation in the integrated peak volumes (Guerrini et al., 2005). For example, in **3,6-CS**, the ratio between 6S/6H was determined by integrating the *O*-6 methylene signals ($\delta_{H,C}$ = 4.23/66.6 and 3.86/60.2), sulfated and non-sulfated glucosamine residues, whereas the ratio between 3S/3H (75:25) was calculated by integrating the signals corresponding to the 3-sulfated and nonsulfated CH at position 3 ($\delta_{H,C}$ = 4.28/80.82 and 3.78/72.8) (Fig. 1b).

Table 1
Sulfation of chitosans.

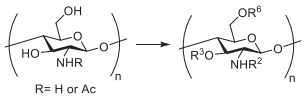

Polysaccharides	R^2	R^3	R^6	Yield	DA[a]	DS[b]
6S-CS	H or Ac	H	SO_3^-	80%	8.0	0.8
3,6S-CS	H or Ac	SO_3^-	SO_3^-	88%	7.2	1.7
3S-CS	H or Ac	SO_3^-	H	57%	9.0	0.7
2S-CS	H or Ac or SO_3^-	H	H	79%	10.5	0.7

Polysaccharides	R^2	R^3	R^6	Yield	DA[a]	DS[b]
6S-CS	H or Ac	H	SO_3^-	80%	8.0	0.8
3,6S-CS	H or Ac	SO_3^-	SO_3^-	88%	7.2	1.7
3S-CS	H or Ac	SO_3^-	H	57%	9.0	0.7
2S-CS	H or Ac or SO_3^-	H	H	79%	10.5	0.7

[a] Degree of acetylation. Calculated according with reference (Jiang et al., 2017).
[b] Total DS_S was determined using elemental analysis.

4. Preparation and characterization of lysozyme-chitosan sulfate hydrogels

Hydrogels were prepared by the Schiff base method using glutaraldehyde as a cross-linking agent (Fig. 2a), and then freeze-dried xerogels were loaded with lysozyme samples. To optimize the preparation procedure, the effects of different parameters (concentrations of chitosan sulfate and GA solutions, pH, and temperature) were analysed. The best experimental conditions (see Section 2.3) were determined based on the swelling ratio, the stability of the hydrogel and the amount of protein absorbed. The appearance of the films of chitosan sulfate hydrogels is shown in Fig. 2b.

The swelling capacity of the hydrogels was evaluated by the degree of swelling (S). Fig. 2c shows the water absorption behaviour of the xerogels at different pH values (3.5, 7.2 and 9.0). The chitosan sulfate-based hydrogels described in this manuscript are polyampholitic systems, due to the presence of amino and sulfate groups, and therefore form networks with oppositely charged structures that can change the charge state of the ionic groups as a function of pH. Since the swelling properties of polyampholite hydrogels are always closely related to the overall charge density and its distribution, we selected two pH values to observe the response of the hydrogels when the amino groups are in the ionized form (NH_3^+) (pH = 3.5) or when the amino groups are deprotonated (pH = 9.0).

For the **CS** hydrogel, the highest degree of swelling was obtained at an acidic pH. The easy uptake of the solution in this hydrogel was attributed to the protonated chitosan amine under these conditions. Thus, when the pH is lower than the pK_a of chitosan (p$K_a \approx 6.20$) (Strand et al., 2001), the amino groups in the chitosan structure are in the ionized form (NH_3^+), which leads to the dissociation of secondary interactions such as intramolecular hydrogen bonds, allowing more water to enter the gel network. This effect is not observed when pH is increased, as amino groups are deprotonated and repulsion in the polymer chains decreases, allowing shrinkage. An opposite effect is observed when chitosan sulfate xerogels are swollen. In this case, the amino groups, when in ionized form, interact strongly with the sulfonic groups ($-SO_3^-$), whose pK_a is nearly 2.60 (Larsson et al., 1981), keeping

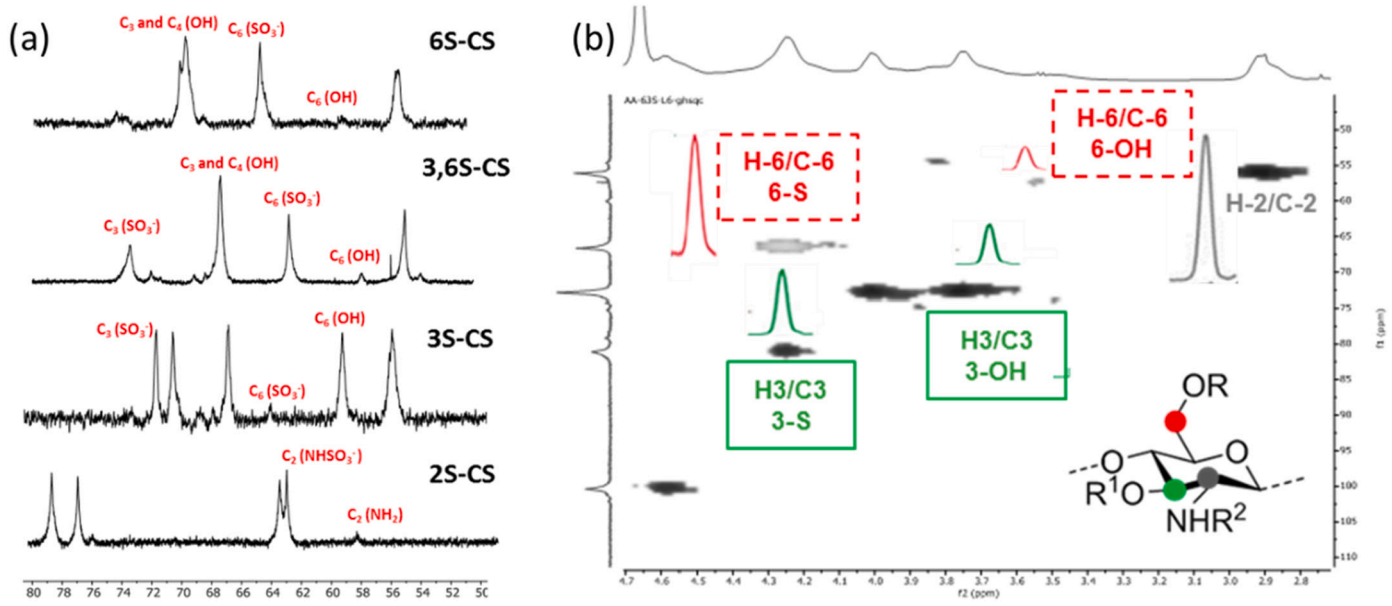

Fig. 1. Characterization of chitosan sulfates. (a) Key regions of the ^{13}C NMR spectra of the polysaccharides **6S-CS**, **3,6S-CS**, **3S-CS**, and **2S-CS** (b) Essential region of the DEPT-HSQC spectra of **3,6S-CS**. The densities in the colour boxes were integrated to estimate the degree of sulfation: 6-position (dashed red line) and 3-position (solid green line).

Table 2
Key signals of ^{13}C NMR spectra of chitosan and chitosan sulfates.

Polysaccharides	Positions					
	$C_2(NH_2)$	$C_2(NHSO_3^-)$	$C_3(OH)$	$C_3(SO_3^-)$	$C_6(OH)$	$C_6(SO_3^-)$
CS	55.2	–	69.8	–	59.3	–
6S-CS	55.9	–	69.9	–	60.2	66.5
3,6S-CS	57.2	–	–	73.9	–	67.7
3S-CS	57.0	–	–	71.3	61.4	–
2S-CS	56.7	63.5	74.5	–	61.8	–

the polymer network shrunk and reducing water uptake. When the pH of the medium is increased, the electronic repulsion between the charged sulfonic groups causes macromolecular expansion and consequently the hydrogels tend to swell more (Durmaz & Okay, 2000; Singh et al., 2011).

Lysozyme was taken up by static absorption at 10 mg/mL in 1.0 mM Tris-HCl buffer (pH = 3.5) until absorption equilibrium was reached (≈72 h), and the concentrations of free lysozyme in the supernatant were measured (Fig. 3a). Although the amount of sulfate groups appears to contribute to the absorption process, the results obtained suggest that other parameters may influence the differences in absorption. Previous results have shown that the lysozyme/chitosan sulfate binding ratios are significantly different depending on the sulfation profile of the polysaccharides (Yuan et al., 2009). To address this question, the binding behaviour of lysozyme with chitosan and its sulfated derivatives in solution was measured in solution. As shown in Fig. 3b, the **3,6S-CS** polysaccharide shows the highest binding activity with lysozyme, while almost half of the lysozyme binds with **6S-CS**. In the case of **2S-CS**, it was observed that mixing the solutions of polysaccharide and lysozyme does not lead to significant flocculation. Although some turbidity is observed, the low values of lysozyme binding with **2S-CS** could be due to the presence of soluble complexes of the polysaccharide with lysozyme, which were not identified in the experiment. A low binding value was observed with **3S-CS** and **CS**. The latter was attributed to the low acetylation degree of the chitosan used, a crucial parameter for the binding of lysozyme to chitosan (Nordtveit et al., 1996). Finally, although the polysaccharide with the highest degree of sulfation (**3,6S-CS**; DS = 1.7) showed the highest binding capacity with lysozyme, the different binding capacities observed for the different monosulfated derivatives (with similar degrees of sulfation) suggest that DS is not the key factor involved in the binding of polysaccharides with lysozyme such as the sulfation profile along the chain.

The mass loss (%) of the hydrogels over time was determined as a measure of degradation (Fig. 3c). Measurable differences in mass were observed depending on the sulfation profile of the polysaccharides used to prepare the hydrogels. For example, the presence of sulfate groups at positions 6 or 2 significantly accelerated the rate of degradation, and after 7 days, approximately 60% and 40% of the mass was lost for the **6S-CS** and **2S-CS** hydrogels, respectively, and at the end of the study (14 days), 80% and 60% of the gel mass was lost for both hydrogels. In contrast, the hydrogels **CS**, **3,6S-CS** and **3S-CS** retained 85%, 75%, and 60%, of their weight respectively, by day 14. The degradation of the hydrogels was examined using cryo-SEM. As shown in Fig. 3d, different pores form in the hydrogel scaffold during lysozyme-mediated degradation. On day 0, both hydrogels (**3S-CS** and **2S-CS**) had comparable pore sizes and size distributions. However, on day 7, although the average pore sizes and size distributions increased for both hydrogels, the **2S-CS** hydrogel showed a greater increase in pore size than the **3S-CS** hydrogel, which was attributed to the greater degradation of the first hydrogel due to the increase in the amount of lysozyme in the hydrogel.

5. In vitro lysozyme release

Fig. 4a shows the cumulative total release of lysozyme as a function of time under neutral conditions (pH = 7.4) for chitosan and chitosan sulfate hydrogels. As can be observed, lysozyme release varies depending on the hydrogel used. There are many mechanisms by which drug

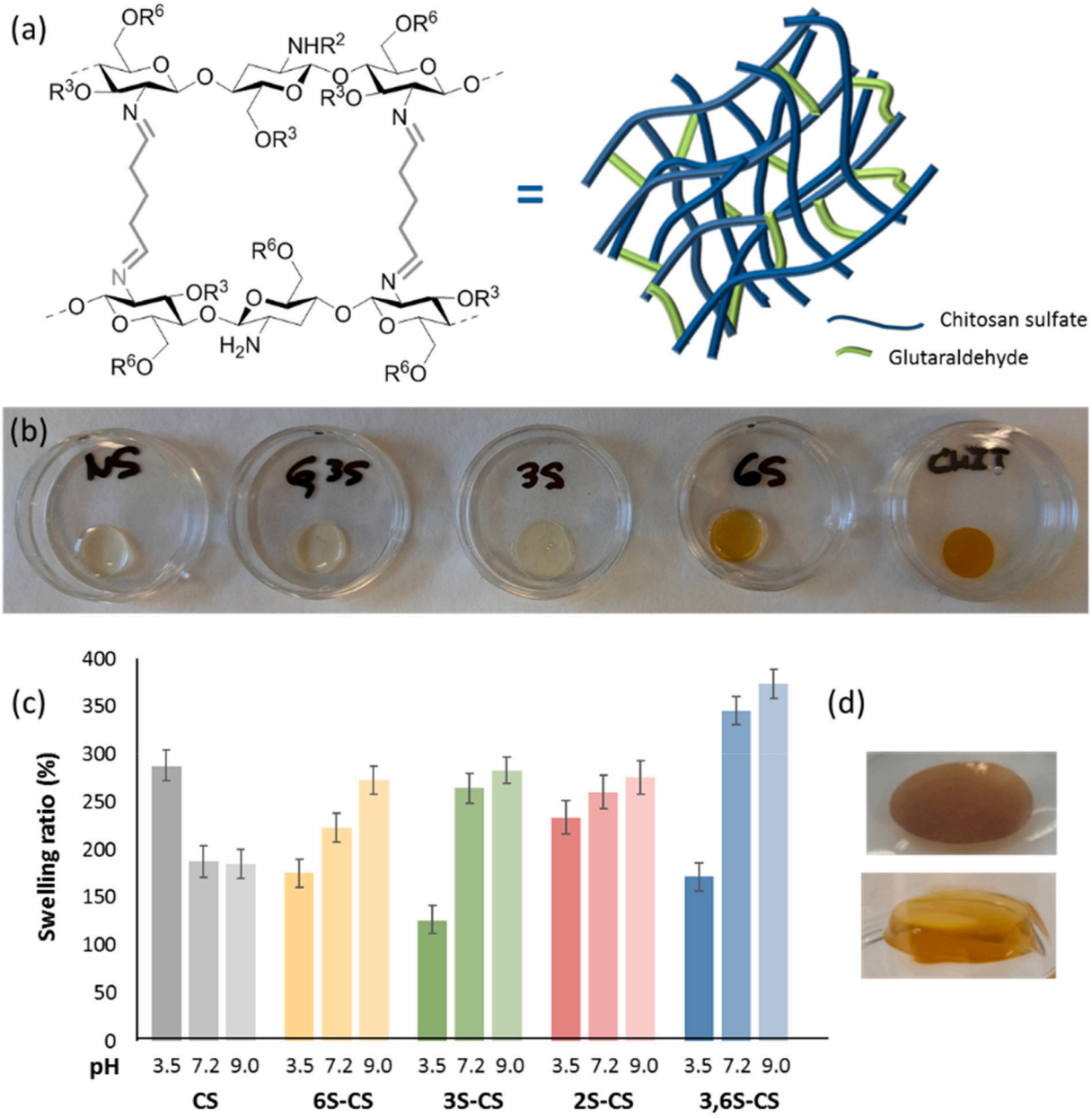

Fig. 2. (a) Molecular structure of cross-linked chitosan sulfate molecules (left) and schematic representation of chitosan sulfate hydrogel networks formed by chemical cross-linking (right). (b) Overall view of chitosan sulfate hydrogels. (c) Swelling ratio of hydrogels calculated by the ratio of wet and dry weights of hydrogels for 48 h at different pH values (3.5, 7.2, and 9.0). Swelling ratios are the average of three replicates and standard deviation are shown. (d) Macroscopic observation of hydrogel swelling over 48 h.

release can be controlled in a system: Dissolution, diffusion, osmosis, partitioning, swelling, degradation, and binding affinity (Bruschi, 2015).

Since our hydrogels were designed with specific ligands for lysozyme recognition, their binding affinities, which depend on the molecular structure of the polysaccharide, could determine the release rate of lysozyme (Yuan et al., 2009). In addition, the incorporated lysozyme could trigger the hydrolysis of the chitosan sulfate, leading to the degradation of the hydrogel and consequent release of the protein (Wang et al., 2012). Finally, it is important to consider that the release of the entrapped lysozyme largely depends on the degree of swelling of the hydrogel. These mechanisms are illustrated in Fig. 4b.

Incubation of the hydrogel **6S-CS** resulted in a biphasic release of lysozyme. Thus, a relatively slow release was observed during the first hours, while a sharp increase in the released lysozyme was observed after this period. This result could be attributed to an increase in the hydrolytic activity of lysozyme after this period. To clarify this behaviour, lysozyme release was analysed at different pH values. When the hydrogel was incubated at a pH of 3.5, only about 15% release was observed after 6 h, whereas at a pH of 9.2, about 82% release was observed after 4 h (Fig. 4c). Considering that chicken egg white lysozyme, the enzyme used in the manuscript, is active in a pH range of 6.0–10.0 and that maximum activity is observed at pH 9.2, it seems clear that the release of lysozyme in **6S-CS** hydrogels could be regulated by the degradation of the hydrogel chains and, consequently, a degradation-controlled release would be the main mechanism for lysozyme release from these hydrogels.

A biphasic release was also observed for the hydrogel **2S-CS**. This hydrogel showed a burst release of about 10% after 6 h, followed by a slow release of about 31% on day 6. After this period, an increase in the

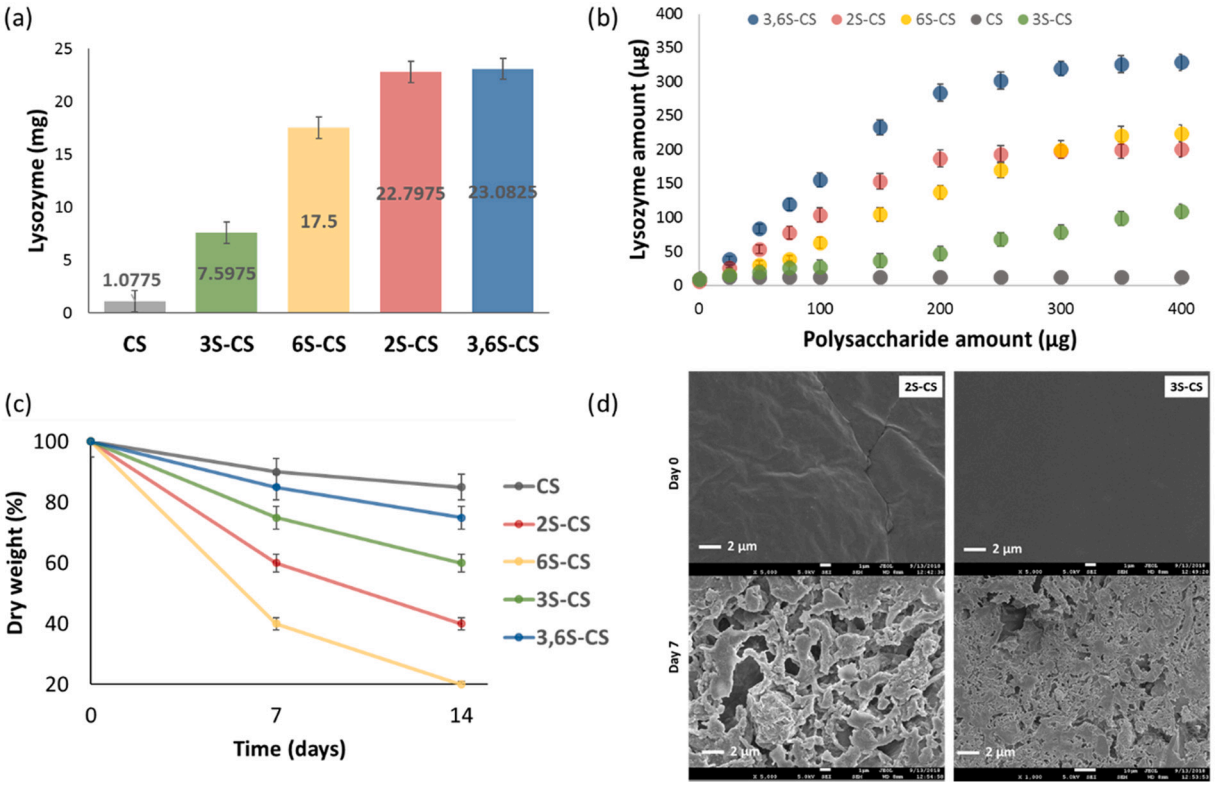

Fig. 3. (a) Quantification of lysozyme loaded in the hydrogels. (b) Binding curves of chitosan sulfates (**3,6S-CS**, **2S-CS**, **6S-CS**, and **3S-CS**) and **CS** with lysozyme. (c) Degradation kinetics of hydrogels for 7 and 14 days by measuring dry weight. (d) Morphological observations of **2S-CS** (left) and **3S-CS** (right) hydrogels by cryo-SEM at days 0 (top) and 7 (bottom). In Fig. 3a, b and c the shown values are the average of three replicates and standard deviations are shown.

amount of lysozyme released is observed. This behaviour could be related to the intrinsic structural properties of the **2S-CS** polysaccharides. While the other polysaccharides have a N substitution degree of about 15%, this degree reaches values of 85% for **2S-CS**. As a result, the available free amino groups are much lower, leading to a lower crosslink density in the formed network. Considering that hydrogels with a higher degree of crosslinking degrade more slowly than hydrogels with a lower degree of crosslinking (Jeon et al., 2007), possible erosion/degradation of the hydrogel over time could be the reason for the observed behaviour.

In contrast, in **3,6S-CS** hydrogels, less than 2% of the encapsulated lysozyme was released within 10 days, indicating that the lysozyme is almost completely entrapped in the hydrogel matrix. This suggests that the release of lysozyme in this case is mainly due to a reaction-diffusion mechanism in which the concentrations of free and bound lysozyme are determined by the equilibrium binding affinity between lysozyme and **3,6S-CS**. Finally, for the hydrogels **3S-CS** and **CS**, after a burst release of about 10% and 7%, respectively, at 3 h, a slow release of 41% and 15% of the total charge was observed after 11 days.

After this period, lysozyme continued to be released (data not shown). After 21 days of incubation, more than 80% of the loaded lysozyme was released in the **2S-CS** and **3S-CS** hydrogels, whereas in the **CS** and **3,6S-CS** hydrogels the cumulative drug release was approximately 20% and 5%, respectively.

To further elucidate the mechanisms hypothesised for each hydrogel, additional experiments were performed. First, the binding affinity between the polysaccharides and lysozyme was analysed by surface plasmon resonance (SPR) (Fig. 5a), and second, the hydrolytic activity of the enzyme towards different polysaccharides was measured (Fig. 5b). The highest binding affinity was observed for **3,6S-CS**, which was about 1.2 and 1.5 times greater than that for **6S-CS** and **2S-CS**, respectively, while the binding affinity for **3S-CS** and **CS** was only about 16% and 4%, respectively, of that of **6S-CS**. In addition, all lysozyme samples bound to chitosan and its sulfated derivatives appeared to show lytic activity after incubation, although the results varied greatly depending on the polysaccharide used. Thus, the lytic activities of the lysozyme bound to **6S-CS** and **3S-CS** were much higher than those bound to the polysaccharides **3,6S-CS** and **2S-CS**, based on the increase in reducing ends observed after 24 h of incubation (1000% and 750% increase for **6S-CS** and for **3S-CS** versus 180% and 350% for **3,6S-CS** and **2S-CS**). The analysis of reducing sugars by DNS-assay was used as an indirect method for the determination of lysozyme activity, because these reducing sugars are formed by the enzymatic cleavage of the glycosidic bond between two glucosamine-chitosan units (McKee, 2017). In this method, the aldehyde functional group of the reducing end of the polysaccharide is oxidized to a carboxyl group, and in the process the yellow 3,5-dintrosalicylic acid compound is reduced to 3-amino, 5-nitrosalicylic acid, which has a reddish-brown colour and can be detected by measuring UV-absorbance of the solution.

These results suggest that although lysozyme recognizes all sulfated polysaccharides, only 6- and 3-sulfation allows a productive binding mode, whereas nonproductive binding occurs when **3,6S-CS** and **2S-CS** are combined with lysozyme. Previous studies have suggested that although the net electrical charge density of the surface (estimated by measuring the ζ-potential) drives the initial interaction between chitosan sulfates and proteins (Doncel-Pérez et al., 2018; Yuan et al., 2009), the unique properties of each protein-chitosan sulfate complex are determined by other polysaccharide features, such as the conformational fit of the polysaccharide to the protein active site (Revuelta et al., 2020). Thus, the ability of **3,6S-CS** and **2S-CS** to bind lysozyme could be explained by the fact that both have the highest net charge on the surface, as shown by their ζ-potential values (Fig. 5c). However, the observed low lysozyme activity suggests that these polysaccharides (**3,6S-CS** and **2S-CS**), unlike **6S-CS** and **3S-CS**, would not allow the molecular conformational adjustment required after the initial ionic interaction. Finally, it is important to note that the sulfate group at

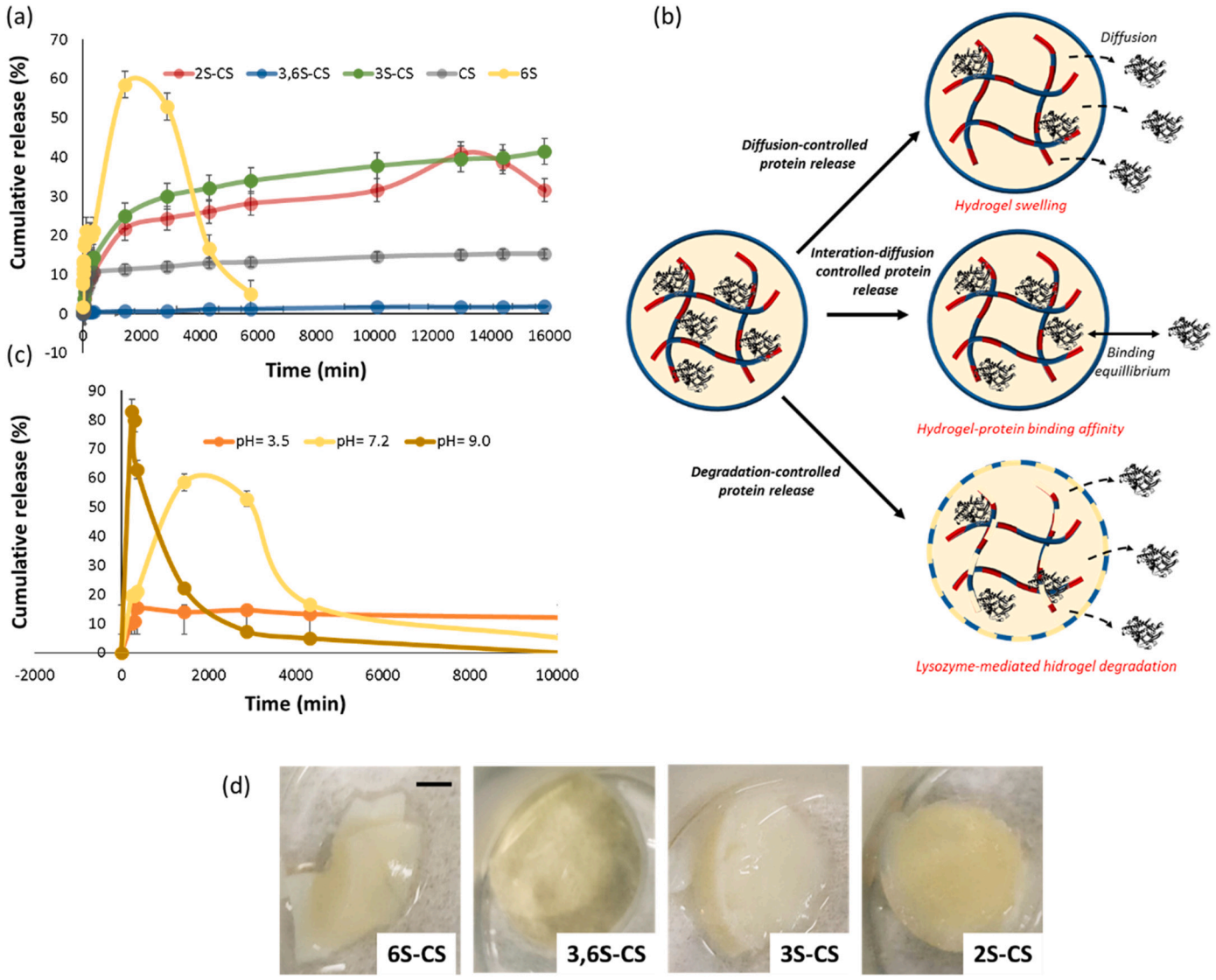

Fig. 4. (a) Lysozyme release profile for chitosan and chitosan sulfate hydrogels; (b) proposed lysozyme release mechanisms for the hydrogels prepared here; (c) lysozyme release profile for **6S-CS** hydrogels at different pH values; (d) macroscopic observation of hydrogels degradation with lysozyme modification for 7 days. Scale bar is 5 mm. Release data are the average of three replicates and standard deviation are shown.

position 3 of chitosan (**3S-CS**) significantly decreases the binding affinity (Fig. 5a) but has little effect on the activity of the bound lysozyme (Fig. 5b). Thus, it appears that lysozyme bound to any of the polysaccharides exhibits high hydrolytic activity regardless of how strong or weak the interaction of lysozyme with **6S-CS** and **3S-CS** polysaccharides is. Finally, the results show no correlation between the activity of lysozyme and the degree of sulfation, since no differences in activity are observed between the most sulfated derivative (3,6S-CS) and the unsulfated CS. Moreover, the monosulfated derivatives exhibit different activities despite their similar degree of sulfation. These results are consistent with observations previously made by other authors (Wang et al., 2012).

These results correlated well with the release behaviour of lysozyme observed with different hydrogels (see Fig. 4a). Consistent with the high hydrolytic activity observed for lysozyme after binding to **6S-CS**, it is plausible to assume that the network structure retains the shape of the native polysaccharide and allows lysozyme to efficiently hydrolyze the hydrogel chains after productive binding, consistent with the previously proposed degradation-controlled release mechanism. A similar mechanism could be attributed to protein release in hydrogel based on **3S-CS**. In contrast, for hydrogels based on **3,6S-CS** and in agreement with the low hydrolytic activity observed for the di-sulfated chitosan-lysozyme complex, it is reasonable to assume that the release mechanism of lysozyme could be controlled by the equilibrium binding affinity between lysozyme and **3,6S-CS**. Since the concentration gradient of the protein is directly determined by its free state, the strong binding reaction between the polysaccharide and lysozyme means that the amount of protein released is very small because it is almost completely entrapped in the hydrogel matrix. A similar release mechanism was proposed for the hydrogel **2S-CS**. However, in this hydrogel, protein release could be more efficient due to the lower affinity for lysozyme-**2S-CS** binding and the high amount of free protein in binding equilibrium. In both cases, the addition of a high concentration of NaCl promoted the release of lysozyme by disrupting the ionic interactions. As shown in Fig. 5d, complete removal of lysozyme from **3,6S-CS** was observed only when a 1.0 M NaCl solution was used, whereas in the **2S-CS** hydrogel, removal was observed when a 0.5 M NaCl solution was used, which could be due to differences in the strength of ionic interactions in each case.

The results described above suggest that the process of release of lysozyme from the developed hydrogels is the result of a combination of different mechanisms due to the presence of various physicochemical

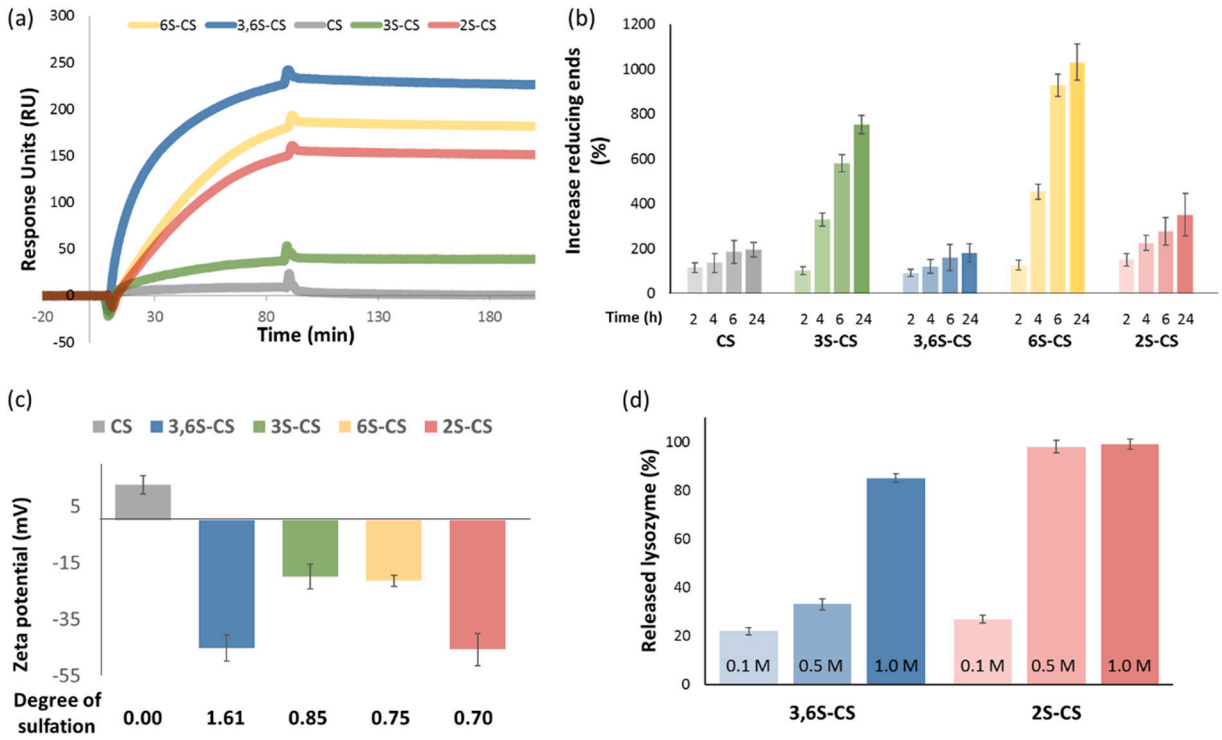

Fig. 5. (a) Binding affinity between polysaccharides and lysozyme analysed by SPR; (b) lytic activity of lysozyme against chitosan and chitosan sulfates determined by measuring the reducing ends; (c) ζ-potential values. Values for the degree of sulfation are shown below. (d) Release of lysozyme from hydrogels in NaCl solutions. In Fig. 5b, c and d the shown values are the average of three replicates and standard deviations are shown.

phenomena (diffusion, swelling, and/or erosion/degradation of the matrix). Although it is difficult to find a mathematical model that describes all the processes that occur, the Korsmeyer-Peppas model has been widely used for systems in which different release mechanisms interact (Korsmeyer et al., 1983; Ilgin et al., 2019). Table 3 shows the estimated parameters after fitting the Korsmeyer-Peppas model to the experimental data. This model uses the value of the release exponent (n), which is the slope of a plot of ln cumulative release versus ln time. When n is 0.5 or less, the release mechanism is theoretically assumed to follow Fick's diffusion for thin films such as the hydrogels prepared here, where drug release occurs by the usual molecular diffusion of a concentration gradient. Higher values of n between 0.5 and 0.1 indicate non-Fickian or anomalous transport, where release is controlled by a combination of diffusion and erosion/degradation of the hydrogel. When n reaches a value of 1.0 or more, the mechanism of release is mainly due to erosion/degradation of the hydrogel (Lao et al., 2011).

As shown in Table 3, application of the lysozyme release data to the Korsmeyer-Peppas model and regression analysis resulted in good fit with coefficients of determination (r^2) greater than 0.94 in all cases. The values for the release exponent (*n*) were 0.105, 0.258, and 0.392 for **CS**, **3S-CS**, and **3,6S-CS** hydrogels, respectively. This indicates that the release of lysozyme from each hydrogel after the initial burst (estimated in 6 h) was controlled by Fick's diffusion through the hydrated matrix. However, for the hydrogel **2S-CS**, the value of *n* was 0.66, indicating that hydrogel degradation cannot be disregarded, although Fick's diffusion is still important. Finally, in the case of the hydrogel **6S-CS**, the value of *n* was 2.50, indicating that the release is completely controlled by the degradation of the network. These results, on the one hand, confirm the existence of different release mechanisms depending on the sulfation profile of the chitosan and, on the other hand, are consistent with the proposed mechanism for each hydrogel based on the experimental data.

Table 3
Values for lysozyme-release profile according to Korsmeyer-Peppas kinetic model.

	Hydrogel				
	2S-CS	**3,6S-CS**	**3S-CS**	**CS**	**6-CS**
n[a]	0.66	0.39	0.25	0.10	2.50
r^2	0.948	0.956	0.962	0.943	0.97
$K_p(h^{-1})$[b]	1.66×10^{-2}	1.69×10^{-2}	1.62×10^{-2}	1.72×10^{-2}	7.8×10^{-2}

[a] Release exponent describing the transport mechanism.
[b] Constant describing the drug-sample interaction.

6. Antimicrobial activity

The antimicrobial activities of the hydrogels against *E. coli* strain K12 were evaluated by quantifying the number of colony-forming units (cfu mL^{-1}) of a culture after treatment with the different hydrogels (Fig. S3). As shown in Fig. 6a, all hydrogels without lysozyme showed activity against *E. coli*. After 24 h of incubation, the inhibition of bacterial growth for the hydrogels based on **CS** was 32%. This inhibition value increased to 47% and 35% when 3,6- and 6-sulfated chitosan hydrogels were analysed, whereas lower inhibition values (25% and 5%, respectively) were obtained for hydrogels based on **3S-CS** and **2S-CS**).

Inhibition of bacterial growth in CS based hydrogels can be explained by their cationic nature. The interaction of cationic polysaccharides such as chitosan with the negatively charged cell wall of bacteria has been described, resulting in increased cell permeability, decreased cell wall integrity, and subsequent leakage of intracellular proteases and other components (Matica et al., 2019). For chitosan sulfates, it seems clear that anionic polysaccharides are unlikely to bind to the negatively charged surface of microorganisms through electrostatic interactions. In recent decades, it has been proposed that bacteria utilize heparan sulfate proteoglycans present on the extracellular matrix to facilitate cell adherence, attachment, and invasion and to evade defense mechanisms (Rostand & Esko, 1997). In particular, heparan sulfates appear to bind bacteria via adhesins, macromolecular components of the bacterial cell

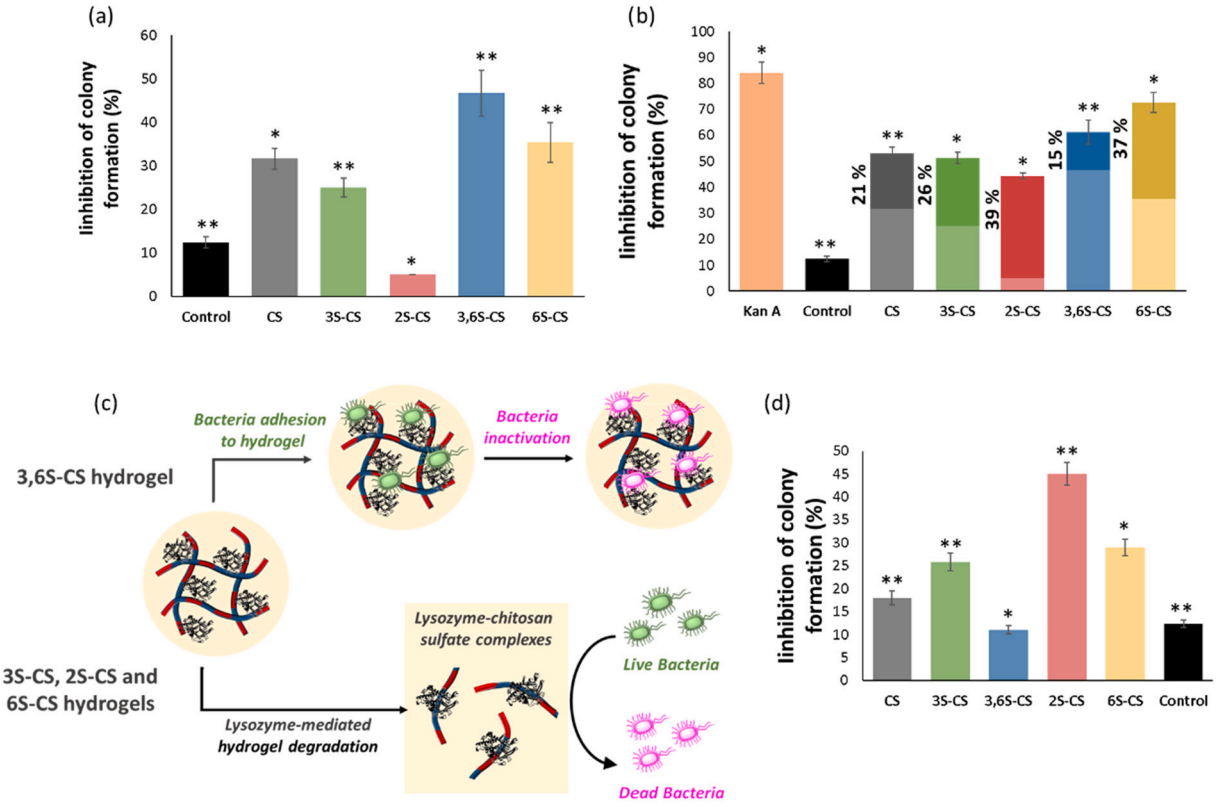

Fig. 6. (a) Percent cfu inhibition of hydrogels without lysozyme; (b) comparison of percent cfu inhibition of hydrogels without lysozyme (shown in light) and lysozyme-incorporated hydrogels (shown in dark). The increase in inhibition after lysozyme incorporation is shown to the left of each bar. Kanamycin A (50 μg/mL) was used as positive control; (c) proposed mechanisms of antibiotic action of hydrogels; (d) percentage cfu inhibition between 48 h and 72 h. *$P < 0.001$ ($n = 3$); **$P < 0.05$ ($n = 3$).

surface that interact with specific target receptors on the host cell (García et al., 2014). On this basis, sulfated polysaccharides in general and chitosan sulfates in particular could target bacterial surface proteins and inhibit the infection process (Liu et al., 2020; Tziveleka et al., 2018). Although further studies are needed, this mechanism could explain the different behaviour observed depending on the sulfation profile of the polysaccharide used to prepare the hydrogel, considering that the sulfation profile could be particularly relevant for the ionic binding between the chitosan sulfates and the bacterial surface proteins, as is the case when these polysaccharides are used as heparanized chitosans mimicking the natural heparan sulfates (Doncel-Pérez et al., 2018; Revuelta et al., 2020, 2021).

All lysozyme-incorporated hydrogels were significantly more effective than hydrogels without lysozyme (Fig. 6b). This increase in antibiotic activity can be attributed to several causes, such as the release of lysozyme, the degradation of the hydrogel by the incorporation of lysozyme, or the change in antibacterial properties of lysozyme when conjugated to the polysaccharides.

Lysozyme (2.0 mg) used as a control inhibited bacterial growth by approximately 12%. The synergistic effect of lysozyme on chitosan-based hydrogels on antimicrobial activity has been described previously and is attributed to a strong surfactant activity of the lysozyme-chitosan conjugate, causing outer membrane disruption and subsequent lysis of the peptidoglycan layer of Gram-negative bacteria (Song et al., 2002; Tan et al., 2014). Thus, one explanation for the observed effect of the lysozyme-incorporated **CS** hydrogel could be that the strong surfactant activity of the lysozyme-chitosan conjugate on the hydrogel surface causes destruction of the outer membrane and subsequent lysis of the peptidoglycan.

Although the exact mechanism of the observed antibacterial effect of chitosan sulfate-based hydrogels is not fully understood, two alternative mechanisms for the antibacterial effect of hydrogels have been proposed based on the results obtained (Fig. 6c).

Previous studies have reported that binding of chitosan sulfates to lysozyme can significantly alter the specific hydrolytic activity of the enzyme with bacterial cell wall components (Wang et al., 2012). The increase in activity observed for 3,6-disulfated chitosan-lysozyme complexes may be the origin of the behaviour observed for **3,6S-CS** lysozyme-incorporated hydrogel. Although the estimated release of lysozyme in 24 h was 10 fold lower than that of the control (0.2 mg versus 2.0 mg), a higher inhibitory effect was observed (15% for the hydrogel versus 12% for the control). In this context, lysozyme could specifically bind to **3,6S-CS** on the hydrogel surface, leading to the formation of a polysaccharide-lysozyme complex with higher specific hydrolytic activity with bacterial cell wall components than free lysozyme (Tan et al., 2014).

The stronger effect of lysozyme was shown in **6S-CS**, **2S-CS** and **3S-CS** hydrogels. In these, lysozyme cleaves the polysaccharide chains, leading not only to degradation of the gel network (see Fig. 3c), but also to the release of significant amounts of lysozyme (see Fig. 4a), which could be the cause of inhibition of bacterial growth. However, the observed antibacterial activities for these hydrogels did not correspond in every case to the superposition effect stimulated by the hydrogels without enzyme and the released lysozyme, with the exception of the **2S-CS** hydrogel. For example, for the **3S-CS** hydrogel the inhibitory effect was more than twice that of the lysozyme control (26% and 12%, respectively), although the estimated amount of lysozyme released into the hydrogel within 24 h was the same that used as the control (2 mg). In contrast, for the hydrogel **6S-CS**, the increase in observed activity was relatively small despite the large amount of lysozyme released. One possible explanation could be that lysozyme-mediated hydrogel degradation leads to the formation of lysozyme-chitosan-sulfate complexes,

which have different antibacterial properties depending on the effects of the different sulfated chitosans on lysozyme activity (Aminlari et al., 2014; Saito et al., 2019; Wang et al., 2012).

For the **6S-CS**, **2S-CS**, and **3S-CS** hydrogels, antibiotic activity could be attributed to the enzymatic activity of lysozyme bound to the products of lysozyme-mediated degradation of the hydrogel. For **2S-CS**, this activity remains almost similar to the native protein after lysozyme binding to 2-*O*-sulfated chains, whereas for **6S-CS**, it decreases significantly after binding to 6-*O*-sulfated chains. In contrast, a synergistic antibacterial effect is observed with **3S-CS**. Binding of **3S-CS** chains to lysozyme not only maintains but even enhances the catalytic activity of lysozyme, allowing efficient digestion of bacterial cell walls.

Finally, the antibacterial efficacy of hydrogels was investigated over a longer period of time. For this purpose, the hydrogels were incubated for 48 h. After this incubation, the hydrogels were incubated again for 24 h in a new bacterial culture. As can be seen in Fig. 6d, all hydrogels retained their efficacy after three days, with different behaviors depending on the hydrogel analysed. The best sustained antibacterial activities were observed for the hydrogels **2S-CS**, **3S-CS** and **6S-CS** (45%, 29%, and 26%, respectively) and could be due to the progressive lysozyme-mediated hydrogel degradation and subsequent release of lysozyme-chitosan sulfate complexes.

In this way, our systems provide not only versatile platforms with tunable properties, such as the rate and mechanism of lysozyme release, but also a potential strategy to enhance the antibiotic activity of lysozyme against Gram-negative bacteria, such as *E. coli*, bacteria in which lysozyme is less active due to the different structure of their cell wall compared to Gram-positive bacteria (Liu et al., 2018b).

7. Antioxidant activity

The antioxidant activity of the hydrogels was analysed using a DPPH radical scavenging assay (Chen et al., 2021). Sulfated CS hydrogels showed greater antioxidant activity than **CS** hydrogel (Fig. 7a). Previous studies have shown that the degree of sulfation is an important parameter for the antioxidant activity of polysaccharides (Chen & Huang, 2019; Zhong et al., 2019). Moreover, in regioselective sulfated derivatives, the best antioxidant effects were observed when 3,6-disulfated chitosan was used (Seedevi et al., 2017; Xing et al., 2005).

Based on the generally accepted notion that the DPPH free radical scavenging by antioxidants is due to their ability as hydrogen donating (Chen & Ho, 1995) and although the mechanism of sulfated chitosans on DPPH should be further investigated, a possible explanation for the differences observed here could be the strong ability of hydrogel **3,6S-CS** to donate hydrogen compared with the other hydrogels. As can be seen in Fig. 7a, the activity of the hydrogels in scavenging DPPH radicals increased with time. The longest time could lead to more active groups hiding inside the hydrogel being exposed to DPPH, which facilitates DPPH radical scavenging (Zhang et al., 2020).

When hydrogels with lysozyme were analysed, the antioxidant activity of **CS** and **3,6S-CS** was similar to that of hydrogels without lysozyme. However, a different behaviour was observed when the antioxidant activities of **3S-CS**, **2S-CS**, and **6S-CS** were measured. In all cases, a significant decrease was observed as time progressed, possibly due to lysozyme-mediated degradation of the hydrogel (results not shown).

To gain insight into this behaviour, the antioxidant activity of the supernatants released from the gel was analysed. As can be seen in Fig. 7b, a small scavenging effect for DPPH was observed for **CS** and **3,6S-CS**, while for **6S-CS**, **2S-CS**, and **3S-CS** the supernatants released from the hydrogels showed greater antioxidant activity compared to the hydrogels. Previous studies have shown that the DPPH radical scavenging activity of chitosan and its derivatives increases with decreasing molecular weight (Avelelas et al., 2019; Kim & Thomas, 2007; Yen et al., 2008). Among the chitosan sulfate derivatives, those with low molecular weight are generally described as more potent antioxidants, which may be due to the ability of these polysaccharides to adopt more ordered and extended structures, as we have previously described (Revuelta et al., 2020).

Based on these previous results, it is reasonable to assume that lysozyme-mediated degradation of the hydrogel resulted in the leaching of smaller polysaccharide fragments, whose antioxidant activity is more pronounced because of the greater accessibility of the reactive groups compared with the less accessible reactive groups inside the hydrogel. The presence of these fragments in the leachate was confirmed by the DMMB assay (Fig. S4). Finally, the sulfation site seems to be of great importance for the antioxidant activity of chitosan sulfate (Xing et al., 2005). On the one hand, and considering that the antioxidant activity of chitooligomers and their derivatives is related to the amount and activity of the hydroxyl group at C-6 and even more to the amino group at C2 of the chitosan molecule (Xie et al., 2001), the substitution of these functional groups in **6S-CS** and **2S-CS** by sulfate groups may decrease the amount of active amino and hydroxyl groups in the polymer chains. In contrast, sulfation of the hydroxyl group at C-3 can partially destroy the inter- and intramolecular interactions of chitosan, resulting in a more ordered and extended structure that could exert the observed high activity. A similar correlation between antioxidant activities and sulfation site has already been observed by other authors (Seedevi et al.,

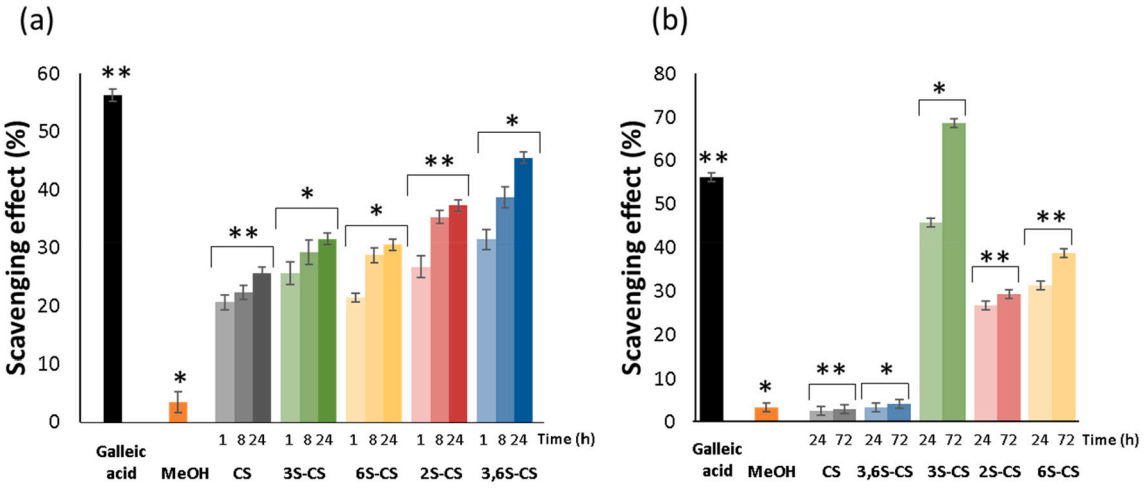

Fig. 7. (a) Scavenging activity of hydrogels without lysozyme after 1, 8 and 24 h; (b) scavenging activity of supernatants after release of lysozyme after 24 and 72 h. Galleic acid (100 mg/mL) and MeOH (50% v/v) have been employed as positive and negative controls respectively. *$P < 0.001$ ($n = 3$); **$P < 0.05$ ($n = 3$).

2017; Xing et al., 2005).

8. Conclusions

In summary, hydrogels have been prepared based on 2-O-sulfated, 3-O-sulfated, 6-O-sulfated, and 3,6-O-disulfated chitosans (CS) and lysozyme. Our study has shown that in these hydrogels, sulfate position along the chitosan chain is the key factor that modulates the behaviour of the hydrogels and provides a versatile platform with fine-tuned degradability and sustained antibiotic and antioxidant activities. Thus, the release of lysozyme in 6S-CS hydrogels could be regulated by the degradation of the hydrogel chains, but in this case of 3,6S-CS hydrogels — which have the highest affinity for lysozyme — the release of lysozyme is mainly controlled by a reaction-diffusion mechanism. On the other hand, the lytic activity of the lysozyme bound on 6S-CS and 3S-CS were much higher than that on the polysaccharides 3,6S-CS and 2S-CS. As for the antioxidant activity, CS and 3,6S-CS hydrogels with lysozyme showed similar activity to that of hydrogels without lysozyme and significantly higher than the antioxidant activity of 3S-CS, 2S-CS and 6S-CS hydrogels with lysozyme.

Therefore, in the hydrogels we developed, both the rate and mechanism of lysozyme release and the antibacterial and antioxidant activities depend only on the positioning of sulfate groups along the chitosan chains, a structural parameter that, unlike the degree and pattern of acetylation, is easily controlled by rapid, inexpensive, simple, and precise chemical modifications. The presented results indicate that the strategy of combining lysozyme with chitosan sulfates is a promising approach that greatly improves the versatility of current chitosan-lysozyme scaffolds.

Finally, and given the structural and functional similarities of chitosan sulfate with heparan sulfates that allow them to affect and modulate both cell morphology and function, thus controlling their proliferation and/or differentiation (Doncel-Pérez et al., 2018; Revuelta et al., 2021), the scaffolds prepared in this manuscript are promising for a range of tissue engineering applications (Zeng et al., 2019; Dinoro et al., 2019). However, studies still need to be conducted to determine the safety of the new hydrogels and evaluate their mechanical properties, among other things. Nevertheless, it is worth noting that previous studies have shown that chitosan-lysozyme hybrid hydrogels crosslinked with glutaraldehyde are not cytotoxic materials (Kim et al., 2018). Together with the non-cytotoxic effects observed for chitosan sulfates (Revuelta et al., 2020), this suggests good safety of our systems. Moreover, the chitosan sulfate-based hydrogels prepared in this manuscript exhibited elastic modulus values that are in the range of other hydrogels that have demonstrated their applicability in the development of scaffolds for tissue engineering (Chen et al., 2013; Markert et al., 2013).

CRediT authorship contribution statement

Antonio Aguanell: Investigation, Methodology, Formal analysis. **María Luisa del Pozo:** Investigation, Methodology, Formal analysis. **Carlos Pérez-Martín:** Investigation. **Gabriela Pontes:** Investigation. **Agatha Bastida:** Writing – review & editing. **Alfonso Fernández-Mayoralas:** Writing – review & editing, Funding acquisition. **Eduardo García-Junceda:** Conceptualization, Supervision, Visualization, Writing – review & editing, Validation. **Julia Revuelta:** Conceptualization, Supervision, Visualization, Writing – original draft, Writing – review & editing, Project administration, Funding acquisition, Validation.

Declaration of competing interest

The authors declare that they have no known competing financial interests or personal relationships that could have appeared to influence the work reported in this paper.

Acknowledgment

The authors gratefully acknowledge the financial support provided by the grant PID2019-105337RB-C21 (MICIN/FEDER).

Appendix A. Supplementary data

Supplementary data to this article can be found online at https://doi.org/10.1016/j.carbpol.2022.119611.

References

Akakuru, O., & Isiuku, B. (2017). Chitosan hydrogels and their glutaraldehyde-crosslinked counterparts as potential drug release and tissue engineering systems - Synthesis, characterization, swelling kinetics and mechanism. *Journal of Physical Chemistry & Biophysics, 7*(3), 1000256.

Alemán, J. V., Chadwick, A. V., He, J., Hess, M., Horie, K., Jones, R. G., Kratochvíl, P., Meisel, I., Mita, I., Moad, G., Penczek, S., & Stepto, R. F. T. (2007). Definitions of terms relating to the structure and processing of sols, gels, networks, and inorganic-organic hybrid materials (IUPAC Recommendations 2007). *Pure and Applied Chemistry, 79*(10), 1801–1829. https://doi.org/10.1351/pac200779101801

Aminlari, L., Hashemi, M. M., & Aminlari, M. (2014). Modified lysozymes as novel broad spectrum natural antimicrobial agents in foods. *Journal of Food Science, 79*(6), R1077–R1090. https://doi.org/10.1111/1750-3841.12460

Avelelas, F., Horta, A., Pinto, L. F. V., Cotrim Marques, S., Marques Nunes, P., Pedrosa, R., & Leandro, S. M. (2019). Antifungal and antioxidant properties of chitosan polymers obtained from nontraditional Polybius henslowii sources. *Marine Drugs, 17*(4), 239. https://doi.org/10.3390/md17040239

Bedini, E., Laezza, A., Parrilli, M., & Iadonisi, A. (2017). A review of chemical methods for the selective sulfation and desulfation of polysaccharides. *Carbohydrate Polymers, 174*, 1224–1239. https://doi.org/10.1016/j.carbpol.2017.07.017

Bruschi, M. L. (2015). Main mechanisms to control the drug release. In *Strategies to Modify the Drug Release from Pharmaceutical Systems* (pp. 37–62). Woodhead Publishing.

Chen, C.-W., & Ho, C.-T. (1995). Antioxidant properties of polyphenols extracted from green and black teas. *Journal of Food Lipids, 2*(1), 35–46. https://doi.org/10.1111/j.1745-4522.1995.tb00028.x

Chen, L., & Huang, G. (2019). Antioxidant activities of sulfated pumpkin polysaccharides. *International Journal of Biological Macromolecules, 126*, 743–746. https://doi.org/10.1016/j.ijbiomac.2018.12.261

Chen, S., Wei, X., Sui, Z., Guo, M., Geng, J., Xiao, J., & Huang, D. (2021). Preparation of antioxidant and antibacterial chitosan film from Periplaneta Americana. In *, Vol. 12. Insects*. https://doi.org/10.3390/insects12010053. Issue 1.

Chen, Z., Wang, W., Guo, L., Yu, Y., & Yuan, Z. (2013). Preparation of enzymatically cross-linked sulfated chitosan hydrogel and its potential application in thick tissue engineering. *Science China Chemistry, 56*(12), 1701–1709. https://doi.org/10.1007/s11426-013-4887-8

Cord-Landwehr, S., Richter, C., Wattjes, J., Sreekumar, S., Singh, R., Basa, S., El Gueddari, N. E., & Moerschbacher, B. M. (2020). Patterns matter part 2: Chitosan oligomers with defined patterns of acetylation. *Reactive and Functional Polymers, 151*, Article 104577. https://doi.org/10.1016/j.reactfunctpolym.2020.104577

Dinoro, J., Maher, M., Talebian, S., Jafarkhani, M., Mehrali, M., Orive, G., Foroughi, J., Lord, M. S., & Dolatshahi-Pirouz, A. (2019). Sulfated polysaccharide-based scaffolds for orthopaedic tissue engineering. *Biomaterials, 214*(December 2018), Article 119214. https://doi.org/10.1016/j.biomaterials.2019.05.025

Domalik-Pyzik, P., Chłopek, J., & Pielichowska, K. (2019). In M. I. H. Mondal (Ed.), *Chitosan-based hydrogels: Preparation, properties, and applications BT - Cellulose-based superabsorbent hydrogels* (pp. 1665–1693). Springer International Publishing. https://doi.org/10.1007/978-3-319-77830-3_55.

Doncel-Pérez, E., Aranaz, I., Bastida, A., Revuelta, J., Camacho, C., Acosta, N., Garrido, L., Civera, C., García-Junceda, E., Heras, A., & Fernández-Mayoralas, A. (2018). Synthesis, physicochemical characterization and biological evaluation of chitosan sulfate as heparan sulfate mimics. *Carbohydrate Polymers, 191*, 225–233. https://doi.org/10.1016/j.carbpol.2018.03.036

Durmaz, S., & Okay, O. (2000). Acrylamide/2-acrylamido-2-methylpropane sulfonic acid sodium salt-based hydrogels: Synthesis and characterization. *Polymer, 41*(10), 3693–3704. https://doi.org/10.1016/S0032-3861(99)00558-3

Eivazzadeh-Keihan, R., Noruzi, E. B., Mehrban, S. F., Aliabadi, H. A. M., Karimi, M., Mohammadi, A., Maleki, A., Mahdavi, M., Larijani, B., & Shalan, A. E. (2022). Review: The latest advances in biomedical applications of chitosan hydrogel as a powerful natural structure with eye-catching biological properties. *Journal of Materials Science, 57*(6), 3855–3891. https://doi.org/10.1007/s10853-021-06757-6

García, B., Fernández-Vega, I., Garcia-suarez, O., Castañón De La Torre, S., & Quirós, L. (2014). The role of heparan sulfate proteoglycans in bacterial infections. *Journal of Medical Microbiology & Diagnosis, 3*. https://doi.org/10.4172/2161-0703.1000157

Guerrini, M., Naggi, A., Guglieri, S., Santarsiero, R., & Torri, G. (2005). Complex glycosaminoglycans: Profiling substitution patterns by two-dimensional nuclear magnetic resonance spectroscopy. *Analytical Biochemistry, 337*(1), 35–47. https://doi.org/10.1016/j.ab.2004.10.012

Gusakov, A. V., Kondratyeva, E. G., & Sinitsyn, A. P. (2011). Comparison of two methods for assaying reducing sugars in the determination of carbohydrase activities.

International Journal of Analytical Chemistry, 2011, Article 283658. https://doi.org/10.1155/2011/283658

Han, Z., Zeng, Y., Zhang, M., Zhang, Y., & Zhang, L. (2016a). Monosaccharide compositions of sulfated chitosans obtained by analysis of nitrous acid degraded and pyrazolone-labeled products. *Carbohydrate Polymers, 136*, 376–383. https://doi.org/10.1016/j.carbpol.2015.07.087

Herdiana, Y., Wathoni, N., Shamsuddin, S., & Muchtaridi, M. (2022). Drug release study of the chitosan-based nanoparticles. *Heliyon, 8*(1), Article e08674. https://doi.org/10.1016/j.heliyon.2021.e08674

Holme, K. R., & Perlin, A. S. (1997a). Chitosan N-sulfate.A water-soluble polyelectrolyte. *Carbohydrate Research, 302*(1–2), 7–12. https://doi.org/10.1016/S0008-6215(97)00117-1

Ilgin, P., Ozay, H., & Ozay, O. (2019). A new dual stimuli responsive hydrogel: Modeling approaches for the prediction of drug loading and release profile. *European Polymer Journal, 113*, 244–253. https://doi.org/10.1016/j.eurpolymj.2019.02.003

Jeon, O., Song, S. J., Lee, K.-J., Park, M. H., Lee, S.-H., Hahn, S. K., Kim, S., & Kim, B.-S. (2007). Mechanical properties and degradation behaviors of hyaluronic acid hydrogels cross-linked at various cross-linking densities. *Carbohydrate Polymers, 70*(3), 251–257. https://doi.org/10.1016/j.carbpol.2007.04.002

Jiang, Y., Fu, C., Wu, S., Liu, G., Guo, J., & Su, Z. (2017). Determination of the deacetylation degree of chitooligosaccharides. *Marine Drugs, 15*(11), 332. https://doi.org/10.3390/md15110332

Kariya, Y., Kyogashima, M., Suzuki, K., Isomura, T., Sakamoto, T., Horie, K., Ishihara, M., Takano, R., Kamei, K., & Hara, S. (2000). Preparation of completely 6-O-desulfated heparin and its ability to enhance activity of basic fibroblast growth factor. *The Journal of Biological Chemistry, 275*(34), 25949–25958. https://doi.org/10.1074/jbc.M004140200

Kim, K. W., & Thomas, R. L. (2007). Antioxidative activity of chitosans with varying molecular weights. *Food Chemistry, 101*(1), 308–313. https://doi.org/10.1016/j.foodchem.2006.01.038

Kim, S., Cui, Z. K., Koo, B., Zheng, J. W., Aghaloo, T., & Lee, M. (2018). Chitosan lysozyme conjugates for enzyme-triggered hydrogel degradation in tissue engineering applications. *ACS Applied Materials & Interfaces, 10*(48), 41138–41145. https://doi.org/10.1021/acsami.8b15591

Kim, S., Fan, J. B., Lee, C. S., & Lee, M. (2020). Dual functional lysozyme-chitosan conjugate for tunable degradation and antibacterial activity. *ACS Applied Bio Materials, 3*(4), 2334–2343. https://doi.org/10.1021/acsabm.0c00087

Korsmeyer, R. W., Gurny, R., Doelker, E., Buri, P., & Peppas, N. A. (1983). Mechanisms of solute release from porous hydrophilic polymers. *International Journal of Pharmaceutics, 15*(1), 25–35. https://doi.org/10.1016/0378-5173(83)90064-9

Kurita, K., Kamiya, M., & Nishimura, S.-I. (1991). Solubilization of a rigid polysaccharide: Controlled partial N-acetylation of chitosan to develop solubility. *Carbohydrate Polymers, 16*(1), 83–92. https://doi.org/10.1016/0144-8617(91)90072-K

Lao, L. L., Peppas, N. A., Boey, F. Y. C., & Venkatraman, S. S. (2011). Modeling of drug release from bulk-degrading polymers. *International Journal of Pharmaceutics, 418*(1), 28–41. https://doi.org/10.1016/j.ijpharm.2010.12.020

Larsson, B., Nilsson, M., & Tjälve, H. (1981). The binding of inorganic and organic cations and H+ to cartilage in vitro. *Biochemical Pharmacology, 30*(21), 2963–2970. https://doi.org/10.1016/0006-2952(81)90260-4

Li, X., Tu, H., Huang, M., Chen, J., Shi, X., Deng, H., Wang, S., & Du, Y. (2017). Incorporation of lysozyme-rectorite composites into chitosan films for antibacterial properties enhancement. *International Journal of Biological Macromolecules, 102*, 789–795. https://doi.org/10.1016/j.ijbiomac.2017.04.076

Liu, H., Wang, C., Li, C., Qin, Y., Wang, Z., Yang, F., Li, Z., & Wang, J. (2018). A functional chitosan-based hydrogel as a wound dressing and drug delivery system in the treatment of wound healing. *RSC Advances, 8*(14), 7533–7549. https://doi.org/10.1039/C7RA13510F

Liu, J., Wang, N., Liu, Y., Jin, Y., & Ma, M. (2018). The antimicrobial spectrum of lysozyme broadened by reductive modification. *Poultry Science, 97*(11), 3992–3999. https://doi.org/10.3382/ps/pey245

Liu, Y., Ma, Y., Chen, Z., Li, D., Liu, W., Huang, L., Zou, C., Cao, M.-J., Liu, G.-M., & Wang, Y. (2020). Antibacterial activity of sulfated galactans from Eucheuma serra and Gracilari verrucosa against diarrheagenic Escherichia coli via the disruption of the cell membrane structure. *Marine Drugs, 18*(8), 397. https://doi.org/10.3390/md18080397

Lončarević, A., Ivanković, M., & Rogina, A. (2017). Lysozyme-induced degradation of chitosan: The characterisation of degraded chitosan scaffolds. *Journal of Tissue Repair and Regeneration, 1*(1), 12–22. https://doi.org/10.14302/issn.2640-6403.jtrr-17-1840

Markert, C. D., Guo, X., Skardal, A., Wang, Z., Bharadwaj, S., Zhang, Y., Bonin, K., & Guthold, M. (2013). Characterizing the micro-scale elastic modulus of hydrogels for use in regenerative medicine. *Journal of the Mechanical Behavior of Biomedical Materials, 27*, 115–127. https://doi.org/10.1016/j.jmbbm.2013.07.008

Matica, M. A., Aachmann, F. L., Tøndervik, A., Sletta, H., & Ostafe, V. (2019). Chitosan as a wound dressing starting material: Antimicrobial properties and mode of action. In. *International Journal of Molecular Sciences, 20*(23). https://doi.org/10.3390/ijms20235889

McKee, L. S. (2017). In D. W. Abbott, & A. L. van Bueren (Eds.), *Measuring enzyme kinetics of glycoside hydrolases using the 3,5-dinitrosalicylic acid assay BT - Protein-carbohydrate interactions: Methods and protocols* (pp. 27–36). Springer New York. https://doi.org/10.1007/978-1-4939-6899-2_3.

Nakal-Chidiac, A., García, O., García-Fernández, L., Martín-Saavedra, F. M., Sánchez-Casanova, S., Escudero-Duch, C., San Román, J., Vilaboa, N., & Aguilar, M. R. (2020). Chitosan-stabilized silver nanoclusters with luminescent, photothermal and antibacterial properties. *Carbohydrate Polymers, 250*, Article 116973. https://doi.org/10.1016/j.carbpol.2020.116973

Nicolle, L., Journot, C. M. A., & Gerber-Lemaire, S. (2021). Chitosan functionalization: Covalent and non-covalent interactions and their characterization. *Polymers, 13*(23), 4118. https://doi.org/10.3390/polym13234118

Nordtveit, R. J., Vårum, K. M., & Smidsrød, O. (1996). Degradation of partially N-acetylated chitosans with hen egg white and human lysozyme. *Carbohydrate Polymers, 29*(2), 163–167. https://doi.org/10.1016/0144-8617(96)00003-3

Peers, S., Montembault, A., & Ladavière, C. (2020). Chitosan hydrogels for sustained drug delivery. *Journal of Controlled Release, 326*, 150–163. https://doi.org/10.1016/j.jconrel.2020.06.012

Pillai, C. K. S., Paul, W., & Sharma, C. P. (2009). Chitin and chitosan polymers: Chemistry, solubility and fiber formation. *Progress in Polymer Science, 34*(7), 641–678. https://doi.org/10.1016/j.progpolymsci.2009.04.001

Pita-López, M. L., Fletes-Vargas, G., Espinosa-Andrews, H., & Rodríguez-Rodríguez, R. (2021). Physically cross-linked chitosan-based hydrogels for tissue engineering applications: A state-of-the-art review. *European Polymer Journal, 145*, Article 110176. https://doi.org/10.1016/j.eurpolymj.2020.110176

Revuelta, J., Aranaz, I., Acosta, N., Civera, C., Bastida, A., Peña, N., Monterrey, D. T., Doncel-Pérez, E., Garrido, L., Heras, Á., García-Junceda, E., & Fernández-Mayoralas, A. (2020a). Unraveling the structural landscape of chitosan-based heparan sulfate mimics binding to growth factors: Deciphering structural determinants for optimal activity. *ACS Applied Materials & Interfaces, 12*(23), 25534–25545. https://doi.org/10.1021/acsami.0c03074

Revuelta, J., Fraile, I., Monterrey, D. T., Peña, N., Benito-Arenas, R., Bastida, A., Fernández-Mayoralas, A., & García-Junceda, E. (2021a). Heparanized chitosans: Towards the third generation of chitinous biomaterials. *Materials Horizons, 8*(10), 2596–2614. https://doi.org/10.1039/D1MH00728A

Revuelta, J., Fraile, I., Monterrey, D. T., Peña, N., Benito-Arenas, R., Bastida, A., Fernández-Mayoralas, A., & García-Junceda, E. (2021b). Heparanized chitosans: Towards the third generation of chitinous biomaterials. *Materials Horizons, 8*(10), 2596–2614. https://doi.org/10.1039/D1MH00728A

Rostand, K. S., & Esko, J. D. (1997). Microbial adherence to and invasion through proteoglycans. *Infection and Immunity, 65*(1), 1–8. https://doi.org/10.1128/iai.65.1.1-8.1997

Saito, H., Sakakibara, Y., Sakata, A., Kurashige, R., Murakami, D., Kageshima, H., Saito, A., & Miyazaki, Y. (2019). Antibacterial activity of lysozyme-chitosan oligosaccharide conjugates (LYZOX) against Pseudomonas aeruginosa, Acinetobacter baumannii and methicillin-resistant Staphylococcus aureus. *PLOS ONE, 14*(5), Article e0217504. https://doi.org/10.1371/journal.pone.0217504

Sanchez-Salvador, J. L., Balea, A., Monte, M. C., Negro, C., & Blanco, A. (2021). Chitosan grafted/cross-linked with biodegradable polymers: A review. *International Journal of Biological Macromolecules, 178*, 325–343. https://doi.org/10.1016/j.ijbiomac.2021.02.200

Seedevi, P., Moovendhan, M., Vairamani, S., & Shanmugam, A. (2017). Evaluation of antioxidant activities and chemical analysis of sulfated chitosan from Sepia prashadi. *International Journal of Biological Macromolecules, 99*, 519–529. https://doi.org/10.1016/j.ijbiomac.2017.03.012

Singh, A., Sarkar, D. J., Singh, A. K., Parsad, R., Kumar, A., & Parmar, B. S. (2011). Studies on novel nanosuperabsorbent composites: Swelling behavior in different environments and effect on water absorption and retention properties of sandy loam soil and soil-less medium. *Journal of Applied Polymer Science, 120*(3), 1448–1458. https://doi.org/10.1002/app.33263

Song, H., Inaka, K., Maenaka, K., & Matsushima, M. (1994). Structural changes of active site cleft and different saccharide binding modes in human lysozyme co-crystallized with hexa-N-acetyl-chitohexaose at pH 4.0. *Journal of Molecular Biology, 244*(5), 522–540. https://doi.org/10.1006/jmbi.1994.1750

Song, Y., Babiker, E. E., Usui, M., Saito, A., & Kato, A. (2002). Emulsifying properties and bactericidal action of chitosan–lysozyme conjugates. *Food Research International, 35*(5), 459–466. https://doi.org/10.1016/S0963-9969(01)00144-2

Strand, S. P., Tømmeraas, K., Vårum, K. M., & Østgaard, K. (2001). Electrophoretic light scattering studies of chitosans with different degrees of N-acetylation. *Biomacromolecules, 2*(4), 1310–1314. https://doi.org/10.1021/bm015598x

Tan, M., Wang, H., Wang, Y., Chen, G., Yuan, L., & Chen, H. (2014). Recyclable antibacterial material: Silicon grafted with 3,6-O-sulfated chitosan and specifically bound by lysozyme. *Journal of Materials Chemistry B, 2*(5), 569–576. https://doi.org/10.1039/C3TB21358G

Tomihata, K., & Ikada, Y. (1997). In vitro and in vivo degradation of films of chitin and its deacetylated derivatives. *Biomaterials, 18*(7), 567–575. https://doi.org/10.1016/S0142-9612(96)00167-6

Torkaman, S., Rahmani, H., Ashori, A., & Najafi, S. H. M. (2021). Modification of chitosan using amino acids for wound healing purposes: A review. *Carbohydrate Polymers, 258*, Article 117675. https://doi.org/10.1016/j.carbpol.2021.117675

Tziveleka, L.-A., Pippa, N., Georgantea, P., Ioannou, E., Demetzos, C., & Roussis, V. (2018). Marine sulfated polysaccharides as versatile polyelectrolytes for the development of drug delivery nanoplatforms: Complexation of ulvan with lysozyme. *International Journal of Biological Macromolecules, 118*, 69–75. https://doi.org/10.1016/j.ijbiomac.2018.06.050

Vårum, K. M., Kristiansen Holme, H., Izume, M., Torger Stokke, B., & Smidsrød, O. (1996). Determination of enzymatic hydrolysis specificity of partially N-acetylated chitosans. *Biochimica et Biophysica Acta (BBA) - General Subjects, 1291*(1), 5–15. https://doi.org/10.1016/0304-4165(96)00038-4

Wang, H. W., Yuan, L., Zhao, T. L., Huang, H., Chen, H., & Wu, D. (2012). Altered enzymatic activity of lysozymes bound to variously sulfated chitosans. *Chinese Journal of Polymer Science, 30*(6), 893–899. https://doi.org/10.1007/s10118-012-1181-8

Wattjes, J., Niehues, A., Cord-Landwehr, S., Hoßbach, J., David, L., Delair, T., & Moerschbacher, B. M. (2019). Enzymatic production and enzymatic-mass spectrometric fingerprinting analysis of chitosan polymers with different nonrandom patterns of acetylation. *Journal of the American Chemical Society, 141*(7), 3137–3145. https://doi.org/10.1021/jacs.8b12561

Wattjes, J., Sreekumar, S., Richter, C., Cord-Landwehr, S., Singh, R., El Gueddari, N. E., & Moerschbacher, B. M. (2020). Patterns matter part 1: Chitosan polymers with non-random patterns of acetylation. *Reactive and Functional Polymers, 151*, Article 104583. https://doi.org/10.1016/j.reactfunctpolym.2020.104583

Weinhold, M. X., Sauvageau, J. C. M., Kumirska, J., & Thöming, J. (2009). Studies on acetylation patterns of different chitosan preparations. *Carbohydrate Polymers, 78*(4), 678–684. https://doi.org/10.1016/j.carbpol.2009.06.001

Xie, W., Xu, P., & Liu, Q. (2001). Antioxidant activity of water-soluble chitosan derivatives. *Bioorganic & Medicinal Chemistry Letters, 11*(13), 1699–1701. https://doi.org/10.1016/S0960-894X(01)00285-2

Xing, R., Yu, H., Liu, S., Zhang, W., Zhang, Q., Li, Z., & Li, P. (2005a). Antioxidant activity of differently regioselective chitosan sulfates in vitro. *Bioorganic and Medicinal Chemistry, 13*(4), 1387–1392. https://doi.org/10.1016/j.bmc.2004.11.002

Yen, M.-T., Yang, J.-H., & Mau, J.-L. (2008). Antioxidant properties of chitosan from crab shells. *Carbohydrate Polymers, 74*(4), 840–844. https://doi.org/10.1016/j.carbpol.2008.05.003

Yuan, L., Yue, Z., Chen, H., Huang, H., & Zhao, T. (2009). Biomacromolecular affinity: Interactions between lysozyme and regioselectively sulfated chitosan. *Colloids and Surfaces B: Biointerfaces, 73*(2), 346–350. https://doi.org/10.1016/j.colsurfb.2009.06.003

Zeng, K., Groth, T., & Zhang, K. (2019). Recent advances in artificially sulfated polysaccharides for applications in cell growth and differentiation, drug delivery, and tissue engineering. *ChemBioChem, 20*(6), 737–746. https://doi.org/10.1002/cbic.201800569

Zhang, K., Helm, J., Peschel, D., Gruner, M., Groth, T., & Fischer, S. (2010a). NMR and FT Raman characterisation of regioselectively sulfated chitosan regarding the distribution of sulfate groups and the degree of substitution. *Polymer, 51*(21), 4698–4705. https://doi.org/10.1016/j.polymer.2010.08.034

Zhang, W., Li, X., & Jiang, W. (2020). Development of antioxidant chitosan film with banana peels extract and its application as coating in maintaining the storage quality of apple. *International Journal of Biological Macromolecules, 154*, 1205–1214. https://doi.org/10.1016/j.ijbiomac.2019.10.275

Zhong, Q., Wei, B., Wang, S., Ke, S., Chen, J., Zhang, H., & Wang, H. (2019). The antioxidant activity of polysaccharides derived from marine organisms: An overview. *Marine Drugs, 17*(12), 674. https://doi.org/10.3390/md17120674